ProNGF increases breast tumor aggressiveness through functional association of TrkA with EphA2

Romain Lévêque, Cyril Corbet, Léo Aubert, Matthieu Guilbert, Chann Lagadec, Eric Adriaenssens, Jérémy Duval, Pascal Finetti, Daniel Birnbaum, Nicolas Magné, et al.

ProNGF increases breast tumor aggressiveness through functional association of TrkA with EphA2

Lévêque Romain[1,2,¥], Corbet Cyril[1,2,¥,§], Aubert Léo[1,2,¥], Guilbert Matthieu[1,2], Lagadec Chann[1], Adriaenssens Eric[1,2], Duval Jérémy[1,2], Finetti Pascal[3], Birnbaum Daniel[3], Magné Nicolas[4,5], Chopin Valérie[2,6], Bertucci François[3], Le Bourhis Xuefen[1,2,#] & Toillon Robert-Alain[1,2,#,*]

[1] Inserm, U908, F-59000 Lille, France,
[2] Univ. Lille, U908 - CPAC - Cell plasticity and Cancer, F-59000 Lille, France,
[3] Département d'Oncologie Moléculaire, Institut Paoli-Calmette, CRCM, UMR1068 Inserm, UMR7258 CNRS, Aix-Marseille Université, 13273 Marseille, France,
[4] Département de Radiothérapie, Institut de Cancérologie Lucien Neuwirth, 42270 Saint Priest en Jarez, France,
[5] Radiobiologie Cellulaire et Moléculaire, EMR3738 - Equipe 4, Faculté de Médecine Lyon-Sud, 69000 Lyon, France,
[6] Université de Picardie, 80000 Amiens, France.

[¥] The authors have equally contributed to this work.
Co-senior authors.
[§] Current address: Pole of Pharmacology and Therapeutics (FATH), Institut de Recherche Expérimentale et Clinique (IREC), UCLouvain, 53 Avenue Mounier B1.53.09, B-1200 Brussels, Belgium.
* Corresponding author: Prof. Robert-Alain Toillon, INSERM U908 "Cell Plasticity & Cancer", Bâtiment SN3, 3ème étage, Cité scientifique, Université Lille 1, 59655 Villeneuve d'Ascq, France. Phone: +33 (0)3 20 43 65 59;
E-mail: robert-alain.toillon@univ-lille.fr

Running title: TrkA/EphA2 functional association in breast cancer cells

Keywords: EphA2, TrkA, proNGF, breast cancer

Financial support

This work was supported by grants from the “Ligue Nationale Contre le Cancer”, “Fondation ARC pour la recherche sur le cancer”, “Groupement des Entreprises Françaises dans la Lutte contre le Cancer (GEFLUC)” and the SIRIC Oncolille.

Abstract: 180 words

Word count: 3775 words (+ 41 references)

Number of figures/tables: 6 figures + 1 table

Highlights

- EphA2 is a key element of proNGF signaling in breast cancer cells
- ProNGF-induced Src activation through EphA2 is independent of TrkA phosphorylation
- TrkA/EphA2 PLA signal is associated with decrease of overall survival in breast cancer

Abstract

ProNGF expression has been linked to several types of cancers including breast cancer, and we have previously shown that proNGF stimulates breast cancer invasion in an autocrine manner through membrane receptors sortilin and TrkA. However, little is known regarding TrkA-associated protein partners upon proNGF stimulation. By proteomic analysis and proximity ligation assays, we found that proNGF binding to sortilin induced sequential formation of the functional sortilin/TrkA/EphA2 complex, leading to TrkA-phosphorylation dependent Akt activation and EphA2-dependent Src activation. EphA2 inhibition using siRNA approach abolished proNGF-stimulated clonogenic growth of breast cancer cell lines. Combinatorial targeting of TrkA and EphA2 dramatically reduced colony formation *in vitro*, primary tumor growth and metastatic dissemination towards the brain *in vivo*. Finally, proximity ligation assay in breast tumor samples revealed that increased TrkA/EphA2 proximity ligation assay signals were correlated with a decrease of overall survival in patients.

All together, these data point out the importance of TrkA/EphA2 functional association in proNGF-induced tumor promoting effects, and provide a rationale to target proNGF/TrkA/EphA2 axis by alternative methods other than the simple use of tyrosine kinase inhibitors in breast cancer.

1. Introduction

Elevated levels of pleiotropic growth factors and their cognate receptor tyrosine kinases (RTK) as well as mutated receptors actively participates to cancer progression and resistance to targeted therapies using tyrosine kinase inhibitors [1,2]. Tumor resistance to specific tyrosine kinase inhibitors may be due to complex cross-talk in terms of receptor interactions and their redundant or diversified downstream signaling partners [1,2]. This underlies the need to better characterize growth factor signaling and RTK cooperation in order to optimize such therapies.

In the case of TrkA signaling networks, elicited by nerve growth factor (NGF), several co-receptors such as $p75^{NTR}$, ErbB2, and Ret-5 [3–5] have been reported to modulate TrkA-induced biological effects. Moreover, sortilin is known to be involved in TrkA signaling networks under proNGF (precursor of NGF) stimulation. Sortilin, a member of the Vps10p-domain proteins, is mainly known to be involved in vesicular trafficking but it also acts as a membrane receptor for neurotensin and proneurotrophins [6,7]. Although recombinant proNGF has been described to directly bind to sortilin, $p75^{NTR}$ and TrkA, it has been found that, in neuron cells, proNGF induces sortilin/$p75^{NTR}$ complex formation, leading to apoptotic cell death [8]. Further study showed that high ratio between $p75^{NTR}$ and TrkA stimulates proNGF-induced neuron apoptosis, while low ratio between $p75^{NTR}$ and TrkA stimulates proNGF-induced survival [9]. ProNGF is also associated with non-neuronal malignancies and its expression has been reported in melanoma, prostate, breast and thyroid cancers [10–13]. In melanoma, proNGF can stimulate cancer cell invasion through $p75^{NTR}$ [12] while in prostate cancer, its expression correlates with aggressiveness and nerve infiltration into the tumor site [11]. In

94 breast cancer, we previously reported high levels of proNGF are correlated with
95 lymph node invasion [10]. In addition, proNGF stimulates breast cancer cell
96 invasion through sortilin and TrkA receptors, independently of $p75^{NTR}$, leading to
97 the subsequent activation of Src and Akt signaling pathways [10].
98 Despite the tumor-promoting effects of proNGF, associated signaling pathways
99 still remain fragmentary. Here, we identified EphA2, a membrane receptor tyrosine
100 kinase, as a key element of the proNGF signaling in breast cancer cells. Moreover,
101 increased TrkA/EphA2 proximity ligation assay signals were correlated with a
102 decrease of overall survival in breast cancer patients, further pointing out the
103 importance of TrkA/EphA2 functional association in proNGF-mediated tumor
104 progression. Thus, our results provide a rationale to target proNGF/TrkA/EphA2
105 axis as a promising therapeutic strategy in breast cancer.
106

2. Materials and Methods

2.1. Cell culture

All breast cancer cell lines were acquired from the American Type Culture Collection (ATCC) except for SUM159-PT, which is from Asterand Bioscience. MDA-MB-231 breast cancer cells stably overexpressing HA-tagged native TrkA (MDA-MB-231 HA-TrkA) or a kinase-dead TrkA were established as previously described [10]. Cells were maintained in Eagle's Minimal Essential Medium (Life Technologies) (MDA-MB-231 and MCF-7 cells), or RPMI 1640 medium (Life Technologies) (HCC-1954, T-47D) supplemented with 10 % inactivated FBS (Fetal Bovine Serum) (Hyclone), 2 mM L-glutamine, 1 % non-essential amino acids, 40 UI/ml penicillin, 40 µg/ml streptomycin, 50 µg/ml gentamycin and ZellShield™ (Biovalley) at 37°C in 5 % CO_2-humidified atmosphere. SUM159-PT were grown in Ham's F12 nutrient mix supplemented with 5 % FBS, 10 mM HEPES, 0.1 % insulin, 1 mg/ml hydrocortisone, 40 UI/ml penicillin, 40 µg/ml streptomycin, 50 µg/ml gentamycin and ZellShield™ (Biovalley) at 37°C in 5 % CO_2-humidified atmosphere. Before treatment, cells were rinsed twice with PBS, left for 24h in culture medium supplemented with 0.1 % FBS, and then treated with recombinant human non-cleavable proNGF (denoted as proNGF and used at 0.5 nM in all the experiments) (Alomone Labs) or recombinant human mature NGF at 16 nM (Alomone labs). For some experiments, cells were pre-incubated for 1h with the TrkA pharmacological inhibitor K252a (10 nM, Calbiochem) or neurotensin (1 µM, R&D systems).

2.2. Transfection

Tumor cells were transfected with 2 nM siRNA using INTERFERin™ transfection reagent (Polyplus transfection) following the manufacturer's instructions. The

siRNA sequences used against EphA2 were: GCAAGGAAGUGGUACUGCUGGACUU (from Eurogentec) or GCGUAUCUUCAUUGAGCUCAA [14] compared to a control siRNA sequence (siGFP) GAUGAACUUCAGGGUCAGCTT. For TrkA, a pool of three siRNA sequences (Eurogentec) was used: GAACCUGACUGAGCUCUAC, UGGAGUCUCUCUCCUGGAA and GCUGCAGUGUCAUGGGCAA.

2.3. Immunoprecipitation and Western blot analysis

Immunoprecipitation and Western blotting experiments were carried out as previously reported [15]. The primary antibodies used for Western blotting were: anti-sortilin (#612101, BD Biosciences), anti-TrkA (ANT-018, Alomone Labs), anti-EphA2 (clone 1E3, Abnova), anti-HA (Covance), anti-phospho-Akt (Ser-473) (#9271), anti-pan-Akt (#4691), anti-phospho-Src (Tyr-416) (#2105), anti-Src (#2109) and anti-phospho-TrkA (Tyr-674/675) (#4621) (Cell Signaling Technology). For immunoprecipitation studies, anti-HA (12CA5, Roche), anti-sortilin (BAF2934, R&D Systems) and anti-EphA2 (clone C-20, Santa Cruz Biotechnologies) were used.

2.4. Nano-LC-MS/MS Q-Star analysis

MDA-MB-231 HA-TrkA cells were treated with proNGF for 5 or 30 min. Total cell lysates were subjected to immunoprecipitation using anti-HA (Covance). Immunoprecipitated proteins were then separated by 10 % SDS-PAGE. After colloidal Coomassie blue staining, bands, which intensities were increased under proNGF stimulation, were cut and peptide digests were extracted from the 1-D gel band and nanoLC-nanoESI-MS/MS analyses were performed on a hybrid quadrupole time-of-flight mass spectrometer (Q-Star, Applied Biosystems)

156 equipped with a nano-electrospray ion source coupled with a nano high pressure
157 liquid chromatography system (LC Packings Dionex) as previously described [16].
158 Identified proteins were classified by Panther software (http://www.pantherdb.org).

159 2.5. *In situ* proximity ligation assay (PLA)

160 Cells grown on acid-washed eight-well glass slides (10^4 cells per well) (Thermo
161 Scientific) in appropriate medium with 5 or 10 % FBS for 24h. After treatment,
162 paraformaldehyde-fixed cells were incubated with 4 % BSA (1h, 20°C) followed by
163 overnight incubation with primary antibodies [mouse anti-HA, 1:50 (Covance); goat
164 anti-sortilin, 1:50 (R&D systems); rabbit anti-EphA2, 1:100 (Cell Signaling
165 Technology), mouse anti-TrkA, 1:50 (Alomone Labs)]. PLA was performed as
166 recommended by manufacturer's instructions. Briefly, slides were incubated with
167 secondary antibodies complexed with complementary nucleotide sequences for
168 2h. The formed DNA circle, resulting from complementary nucleotides was then
169 amplified using fluorescent oligonucleotides. Nuclei were counterstained with
170 Hoechst 33258 (Sigma-Aldrich) and samples were mounted with fluorescence
171 mounting medium (Dako). PLA images (fluorescent red dots) were acquired using
172 a fluorescence microscope (100X oil immersion objective, $\lambda_{excitation}$: 562 nm,
173 $\lambda_{emission}$: 624 nm, microscope Eclipse Ti; Nikon) and analyzed with NIS-Elements
174 BR software (Nikon) and Image J.

175 Tissue microarrays were from SuperBioChips (CBA4) and US BioMax (HBre-
176 Duc150Sur01) allowing analysis in 189 individual tumor samples. For PLA in
177 paraffin-embedded patient tumor samples, primary antibodies anti-TrkA (ANT-018,
178 Alomone Labs) and anti-EphA2 (AF3035, R&D systems) were incubated overnight
179 at 4°C. Subsequent steps were done according to the manufacturer's instructions.
180 Briefly, slides were incubated with secondary antibodies complexed with

complementary nucleotide sequences for 2h. The formed DNA circle, resulting from complementary nucleotides was then amplified using oligonucleotides labeled with horseradish peroxidase. PLA signal was evaluated according to the number of dots per cell and the number of stained cells in a double-blind analysis (by TRA and DJ). PLA signal <2 dots/cell was considered as low, PLA signal between 2-10 dots/cell was considered as medium, PLA signal >10 dots/cell was considered as high. Kaplan-Meier curves were obtained by using GraphPad Prism software.

2.6. Clonogenic cell growth

Clonogenic assays were performed as previously described [15]. After siRNA transfection, 2000 cells were seeded in 35 mm Petri dishes and treated with proNGF for 10 days. Colonies were then stained with crystal violet before counting.

2.7. *In vivo* experiments

All the experiments involving mice received the approval of the local ethic committee and were carried out according to French national animal care regulations. MDA-MB-231 HA-TrkA cells ($3x10^6$) were subcutaneously injected into six-week old female SCID mice. Two weeks after cell injection, mice were randomized into four groups (n=7), and were treated a total of three times at 3-day intervals. Lestaurtinib (CEP-701; Calbiochem) was suspended in vehicle (40% polyethylene glycol 1000, 10% povidone C30 and 2% benzyl alcohol in distilled water) and injected intraperitoneally (10 mg/kg). siEphA2 (Eurogentec; 7.5 µg/mouse) was delivered using *in vivo* jetPEI® according to the manufacturer's instructions (Polyplus transfection) and injected subcutaneously near the tumor

mass. Tumor volume was determined throughout the experiment by measuring the length (l) and width (w) and then calculated as $\pi/6 \times l \times w \times (l+w)/2$.

For analyses of breast cancer cell dissemination in mice, xenograft experiments were conducted using MDA-MB-231 HA-TrkA cells. The tumors were allowed to develop for 14 days and the mice were then submitted to 5 injections (every 3 days) of either scrambled siRNA, or TrkA- and EphA2-targeting siRNAs alone or in combination (7.5 µg siRNA/mouse). Tumor volume was determined throughout the experiment by measuring the length (l) and width (w) and tumors were allowed to grow up to 2 cm^3 to allow metastasis of cancer cells. After animal sacrifice, lungs, liver and brain were collected and detection of cancer cells in those organs was carried out by evaluating human microglobulin mRNA expression by RT-PCR as previously described [17].

2.8. Statistical analysis

Results are expressed as mean ± SEM of at least three independent experiments. Two-tailed unpaired Student t-tests, one-way or two-way ANOVA tests (Bonferroni's post-hoc test) and Mann-Whitney tests were used where appropriate.

3. Results

3.1. TrkA is associated with sortilin and EphA2 in proNGF-treated MDA-MB-231 breast cancer cells

In order to decipher TrkA signaling partners under proNGF stimulation, we first performed proteomic analysis in MDA-MB-231 breast cancer cells stably expressing HA-tagged TrkA [10]. Proteins co-immunoprecipitated with HA-TrkA were identified by mass spectrometry analysis (Figure 1). Individual proteins (985) were identified in selected bands from cells treated with proNGF (5 and 30 min) (Figure 1A). Using Panther classification software, we observed that most of the identified proteins were implicated in maturation and vesicular trafficking (binding and catalytic activities). Seven percent were related to membrane receptor and signaling (Figure 1B). As expected, sortilin, the known receptor of proNGF was found to be co-immunoprecipitated with HA-TrkA (Figure 1C). Interestingly, we found that EphA2, a membrane receptor tyrosine kinase, was also co-immunoprecipitated with HA-TrkA. EphA2 is of particular interest, as it is known to be expressed in breast cancer in which it favors aggressive behavior and metastases formation [18]. We also identified Src, cortactin and p130 Cas (BCAR1, *Breast cancer anti-estrogen resistance protein 1*), which are reported to act as early effectors in EphA2 downstream signaling pathways [19]. Other proteins such as SHEP1 (SH2D3C, *SH2 domain-containing protein 3C*), PTP-PEST (PTPN12, *Tyrosine-protein phosphatase non-receptor type 12*) and RIL (PDLI4, *PDZ and LIM domain protein 4*) were also found to be pulled-down with TrkA; these proteins are well known to regulate Src and/or p130 Cas-mediated signaling pathways [20–22]. The other identified proteins including Lasp1 (*LIM and SH3 domain protein 1)*, SNAP23 (*Synaptosomal-associated protein 23),* FHL2 (*Four and a half LIM domains protein 2*), HAX1 (*HCLS1-associated protein X-1)*,

248 adducin, MARCKS (*Myristoylated alanine-rich C-kinase substrate)* gelsolin, and
249 integrins $\alpha_3\beta_1$ are downstream targets of Src and p130 Cas, which are associated
250 with cytoskeleton remodeling and cell migration [23–28].
251 To confirm proNGF-induced TrkA association with sortilin and EphA2 in breast
252 cancer cells, we further performed immunoprecipitation assays by using antibodies
253 against HA (-TrkA), sortilin and EphA2, followed by Western blot analysis (Figure
254 2A). In the absence of proNGF, none of the three receptors was found to be co-
255 immunoprecipitated. Upon proNGF treatment, sortilin and EphA2 were co-
256 immunoprecipitated with TrkA. These results were confirmed by reverse co-
257 immunoprecipitation of sortilin and EphA2 (Figure 2A). Of note, in the presence of
258 NGF, sortilin binding to TrkA was detected after 30 min of treatment but EphA2
259 binding was not observed after neither 5 min nor 30 min of treatment (Figure 2A).
260 Thus, NGF seemed to induce a late TrkA/sortilin association, suggesting that
261 sortilin acts as an endocytic receptor, as previously reported in neuronal cell
262 models [8]. Proximity ligation assays (PLA) were then carried out to confirm any
263 receptor association (distance <40 nm) at the plasma membrane. In the absence
264 of exogenous proNGF stimulation, a basal PLA signal (red dots) was observed for
265 sortilin/TrkA (Figure 2B-C) and TrkA/EphA2 (Figure 2D-E). ProNGF stimulation (5
266 min) enhanced PLA signals of sortilin/TrkA and EphA2/TrkA (Figure 2C and 2E);
267 this increase was transient as membrane PLA signals decreased to basal levels
268 after 30 min of proNGF treatment.
269 Together, these data indicated that proNGF specifically induces the association of
270 TrkA with sortilin and EphA2, even if we cannot exclude the existence of other
271 intermediary partners.

3.2. Sequential sortilin/TrkA/EphA2 association induces TrkA-dependent Akt phosphorylation and EphA2-dependent Src phosphorylation

In order to put insight into the dynamics of the receptors association, we first treated cells with neurotensin that inhibits, by competition, proNGF binding to sortilin [8]. As shown in Figure 3A, in the presence of neurotensin, TrkA was not immunoprecipitated with either sortilin or EphA2, indicating that proNGF binding to sortilin was necessary for sortilin/TrkA/EphA2 association. When TrkA expression was silenced by siRNA (Figure 3B, S1), sortilin did not pull-down EphA2, indicating that sortilin could not associate with EphA2 in the absence of TrkA; this was further confirmed by PLA, as no signal was detected for sortilin/EphA2.

Interestingly, in cells stably expressing a kinase-dead TrkA that prevents receptor phosphorylation (Figure 3D), proNGF still induced TrkA association with sortilin and EphA2, suggesting that TrkA phosphorylation was not necessary for sortilin/TrkA/EphA2 association. Finally, when EphA2 expression was silenced by siRNA (Figure 3E), TrkA and sortilin were co-immunoprecipitated in proNGF-treated cells, indicating that EphA2 was not required for TrkA and sortilin association.

Together, these results suggested that proNGF binding to sortilin elicits sortilin association with TrkA, which in turn recruits EphA2 at cell surface.

As we have previously shown that proNGF stimulates breast cancer cell invasion through TrkA activation, we asked if EphA2 could be involved in TrkA-mediated cell invasion. When EphA2 expression was inhibited by siRNA approach, proNGF was no longer able to stimulate cell invasion both in native and HA-TrkA over-expressing MDA-MB-231 cells (Figure S2), implying that EphA2 was necessary for proNGF-stimulated and TrkA-mediated cell invasion. ProNGF-stimulated invasion

297 implicates the activation of downstream signaling pathways including Akt and Src
298 [10]. On the other hand, Src is also a downstream effector of EphA2 [19], we then
299 determined the respective role of TrkA and EphA2 in Akt and Src activation by
300 using a kinase-dead mutant of TrkA (Figure 3F) or siEphA2 approach (Figure 3G).
301 Following proNGF treatment, Akt was not phosphorylated in cells expressing a
302 kinase-dead mutant of TrkA while Src phosphorylation was maintained (Figure
303 3F), indicating that Akt phosphorylation depended upon TrkA phosphorylation
304 while Src phosphorylation did not. By contrary, in cells transfected with siEphA2,
305 proNGF still induced Akt phosphorylation but not that of Src, indicating that Akt
306 phosphorylation did not depend on EphA2 while Src activation did (Figure 3G).
307 Collectively, our data showed that, in MDA-MB-231 breast cancer cells, proNGF
308 binding to sortilin induced functional sortilin/TrkA/EphA2 association, leading to
309 TrkA-dependent Akt phosphorylation and EphA2-dependent Src phosphorylation
310 (Figure 3H).
311
312 3.3. ProNGF increases breast cell clonogenic growth through functional
313 association of TrkA with EphA2
314 In order to determine the relevance of TrkA/EphA2 functional association in breast
315 cancer cells, we further extended our study on a panel of representative breast
316 cancer cell lines including basal-like (wild type MDA-MB-231, SUM159-PT),
317 luminal-like (MCF-7, T-47D), and HER2-overexpressing basal-like cell line HCC-
318 1954. PLA signals of TrkA/EphA2 were increased after 5 min of stimulation with
319 proNGF in all cell lines tested, except for MCF-7 (Figures 4A and S3). Clonogenic
320 assays were then carried out to evaluate the impact of EphA2 invalidation on
321 proNGF-stimulated cell growth. As shown in Figure 4B, proNGF stimulated
322 clonogenic cell growth in all the cell lines tested; siEphA2 totally abolished

proNGF-induced cell growth except in MCF-7, this was consistent with the results of PLA assay revealing that proNGF did not increase TrkA/EphA2 complex in these cells and with the fact that MCF-7 cells express low levels of both TrkA and EphA2 compared to the other cell lines (Figure S4). Use of another siEphA2 sequence [14] confirmed also the implication of EphA2 in pro-NGF induced clonogenic growth of MDA-MB-231 cells (Figure S5). These results indicated that proNGF-induced cell growth involved TrkA/EphA2 association in different cell lines whatever their molecular classification (*i.e.* basal, luminal or HER2-like). We then examined the impact of TrkA and/or EphA2 inhibition on colony formation in MDA-MB-231 cells. As shown in Figure 4C, the TrkA inhibitor K252a inhibited colony formation to about 85 % of control, siEphA2 to 60 % of control, while combinatory treatment with K252a and siEphA2 inhibited colony formation to less than 30 % of control.

3.4 Simultaneous targeting of TrkA and EphA2 reduces tumor growth and brain metastasis *in vivo*

Given the above results indicating the importance of proNGF-induced TrkA/EphA2 association in breast cancer cells, we determined the potential benefit of a combinatorial targeting of TrkA and EphA2 in xenograft mouse model. As shown in Figure 5A and B, CEP-701 (clinical derivative of K252a) alone did not significantly reduce tumor growth, while siEphA2 alone delayed tumor growth when compared to the control group (scrambled siRNA). Combined treatment of CEP-701 and siEphA2 resulted in a dramatic reduction of tumor burden when compared to CEP-701 or siEphA2 treatment alone. We then evaluated the impact of TrkA and/or EphA2 invalidation on breast cancer cell dissemination in different organs

348 including lungs, liver and brain (Figure 5C). In these conditions, we first confirmed
349 that combined inhibition of TrkA and EphA2 inhibited tumor growth as the median
350 survival of the mice was increased: Median of survival were 40 days in control
351 group, 53 days in siTrkA group, 49 days in siEphA2 group and 57.5 days in siTrkA
352 and siEphA2 mice (Figure S6). We found that tumor cells disseminated readily in
353 these three distant organs. Lung metastasis was not modified under any
354 invalidation condition. Interestingly, TrkA invalidation alone was sufficient to
355 reduce liver metastasis while combined inhibition of TrkA and EphA2 was required
356 to decrease brain metastasis. These results indicated that simultaneous inhibition
357 of TrkA and EphA2 was not only efficient in inhibiting primary tumor growth, but
358 also in reducing brain metastasis formation.

359

360 3.5. ProNGF-induced TrkA/EphA2 association is correlated with poor prognosis in
361 breast cancer

362 To go further on the significance of TrkA/EphA2 functional complex in breast
363 cancer, we performed immunostainings of TrkA, EphA2, and PLA labeling to
364 colocalize TrkA/EphA2 in breast tumor samples in a tissue microarray (TMA)
365 cohort of 189 patients (Figure 6, Table 1 and S1). We found that TrkA expression
366 was associated with PR-negative status (Table 1). However, neither TrkA nor
367 EphA2 alone correlated with overall survival of patients (Figure 6A-H and Table 1).
368 By PLA, we distinguished the differential PLA signals of TrkA/EphA2 in the
369 samples, and found that high level of TrkA/EphA2 PLA signals in tumors was
370 correlated with a significant decrease of overall survival of patients (Figure 6I-L).

371

4. Discussion

Compelling evidences showed that proNGF is more than just a metabolic precursor of NGF, as it exhibits biological activities in a wide range of normal and neoplastic tissues, including breast cancer [6,8–13,17]. Nevertheless, proNGF functions in cells are still in debate due to its pro-survival and pro-apoptotic activities, according to cell types. A recent study reconciled these findings by showing that these opposite biological effects depend on TrkA levels [29]. Indeed, the authors showed that proNGF elicits apoptotic signaling in PC-12 cells expressing low levels of TrkA while it favors survival of cells expressing high levels of TrkA. In agreement with these findings, increased levels of TrkA are associated with tumor growth and metastasis in breast cancer [30] and melanoma [31].

In breast cancer cells, we previously observed that uncleavable proNGF induces sortilin recruitment at plasma membrane and TrkA activation, leading to increased cell invasion, independently of $p75^{NTR}$ [10]. Herein, by studying TrkA-interacting proteins upon proNGF stimulation, we identified EphA2, a membrane receptor tyrosine kinase, as a key element of proNGF signaling in breast cancer cells. ProNGF signaling through sortilin and TrkA allowed for EphA2 recruitment, which in turn activated Src in a TrkA phosphorylation-independent manner.

Implications of EphA2 in proNGF-induced signaling is of particular interest. Indeed, EphA2 binds to its ligand ephrin-A1 to maintain cell adhesion and tissue homeostasis in normal breast epithelial cells [32], ephrin-A1 downregulation favors ligand-independent activation of EphA2 and associated downstream signaling pathways (*e.g.* MAP-kinase, RhoGTPase and Src) in several types of cancer cells, leading to cell invasion and metastasis [33–35]. Although the mechanisms of ligand-independent activation of EphA2 remain fragmentary, it has been shown

that EphA2 phosphorylation by Akt or Rsk can lead to its activation [35,36]. Here, we observed that in the context of proNGF stimulation, EphA2 activated Src *via* an Akt-phosphorylation independent mechanism. Moreover, our proteomic analysis revealed that several Src-associated signaling proteins like cortactin and p130 Cas were pulled-down with TrkA upon proNGF treatment, suggesting that proNGF could activate a signaling cascade involving Src/p130 Cas/cortactin complex. Although further study should be done to confirm this hypothesis, the Src/p130 Cas/cortactin complex is already reported to induce cell invasion [37].

Song *et al.* [14] have recently reported that EphA2 is overexpressed in the basal-like breast cancer molecular subtype and this overexpression is correlated with poor recurrence-free survival in triple-negative breast cancers. Loss of EphA2 function in both human and genetically engineered mouse models of triple negative breast cancers reduced tumor growth. Herein, we observed that EphA2 silencing inhibited proNGF-stimulated clonogenic cell growth of not only triple negative, but also luminal ER-positive and HER2-positive breast cancer cell lines. This implies that EphA2 is involved in proNGF-stimulated clonogenic cell growth, independently of molecular subtypes. Consistently, we could not find any significant correlation between TrkA/EphA2 complex or co-localization and different subtypes of breast cancer. Of importance, the level of TrkA/EphA2 co-localization is significantly correlated with poor overall survival of patients suffering from breast cancer regardless the cancer subtype, suggesting the potential involvement of proNGF/TrkA/EphA2 axis in breast cancer progression whatever the cancer subtype. These findings reinforced our previous results showing a significant correlation between the expression of proNGF and lymph node invasion [10].

Cross-talk in growth factor-induced signaling pathway is a leading cause of resistance to targeted therapies [38,39]. EphA2 was identified to mediate resistance to multiple targeted therapies including trastuzumab (HER-2 inhibitor) *via* Src activation in breast cancer cells [40], as well as erlotinib (EGFR inhibitor) in lung cancer models [41]. We postulate that the existence of a proNGF-induced EphA2-Src pathway, independently of TrkA phosphorylation and Akt activation, may contribute to tumor resistance to therapies targeting TrkA kinase domain (lestaurtinib, larotrectinib, entrectinib…). Here, we showed that simultaneous targeting of TrkA and EphA2 receptors, dramatically reduced colony formation *in vitro* and tumor development *in vivo*, suggesting that inhibiting both TrkA- and EphA2-dependent signaling pathways may improve the therapeutic benefit in patients (over)expressing TrkA, EphA2 and proNGF.

In conclusion, our data demonstrated that functional interactions between sortilin, TrkA and EphA2 are essential for the tumor-promoting effect of proNGF in breast cancer. Although further translational work is required, our results suggest that proNGF/TrkA/EphA2 axis could be used as both a prognostic marker and a potential therapeutic target in breast cancer.

Acknowledgments

We thank Anne-Sophie Lacoste who performed the mass spectrometry analysis (Mass Spectrometry facility, IFR-147, University Lille, France). We also thank the animal facility at the Pasteur Institute of Lille (PLETHA) for animal housing (Dr J.P. de Cavel, M T Chassat).

Conflicts of interest

All authors declare no conflict of interest

Reference

[1] T.R. Wilson, J. Fridlyand, Y. Yan, E. Penuel, L. Burton, E. Chan, J. Peng, E. Lin, Y. Wang, J. Sosman, A. Ribas, J. Li, J. Moffat, D.P. Sutherlin, H. Koeppen, M. Merchant, R. Neve, J. Settleman, Widespread potential for growth-factor-driven resistance to anticancer kinase inhibitors, Nature. 487 (2012) 505–509. doi:10.1038/nature11249.

[2] S. Gusenbauer, P. Vlaicu, A. Ullrich, HGF induces novel EGFR functions involved in resistance formation to tyrosine kinase inhibitors, Oncogene. 32 (2013) 3846–3856. doi:10.1038/onc.2012.396.

[3] B.L. Hempstead, D. Martin-Zanca, D.R. Kaplan, L.F. Parada, M.V. Chao, High-affinity NGF binding requires coexpression of the trk proto-oncogene and the low-affinity NGF receptor, Nature. 350 (1991) 678–683. doi:10.1038/350678a0.

[4] B.A. Tsui-Pierchala, J. Milbrandt, E.M. Johnson, NGF utilizes c-Ret via a novel GFL-independent, inter-RTK signaling mechanism to maintain the trophic status of mature sympathetic neurons, Neuron. 33 (2002) 261–273.

[5] C. Festuccia, G.L. Gravina, P. Muzi, D. Millimaggi, V. Dolo, C. Vicentini, C. Ficorella, E. Ricevuto, M. Bologna, Her2 crosstalks with TrkA in a subset of prostate cancer cells: rationale for a guided dual treatment, Prostate. 69 (2009) 337–345. doi:10.1002/pros.20884.

[6] O. Clewes, M.S. Fahey, S.J. Tyler, J.J. Watson, H. Seok, C. Catania, K. Cho, D. Dawbarn, S.J. Allen, Human ProNGF: biological effects and binding profiles at TrkA, P75NTR and sortilin, J. Neurochem. 107 (2008) 1124–1135. doi:10.1111/j.1471-4159.2008.05698.x.

[7] D. Feng, T. Kim, E. Ozkan, M. Light, R. Torkin, K.K. Teng, B.L. Hempstead, K.C. Garcia, Molecular and structural insight into proNGF engagement of p75NTR and sortilin, J. Mol. Biol. 396 (2010) 967–984. doi:10.1016/j.jmb.2009.12.030.

[8] A. Nykjaer, R. Lee, K.K. Teng, P. Jansen, P. Madsen, M.S. Nielsen, C. Jacobsen, M. Kliemannel, E. Schwarz, T.E. Willnow, B.L. Hempstead, C.M. Petersen, Sortilin is essential for proNGF-induced neuronal cell death, Nature. 427 (2004) 843–848. doi:10.1038/nature02319.

[9] R. Masoudi, M.S. Ioannou, M.D. Coughlin, P. Pagadala, K.E. Neet, O. Clewes, S.J. Allen, D. Dawbarn, M. Fahnestock, Biological activity of nerve growth factor precursor is dependent upon relative levels of its receptors, J. Biol. Chem. 284 (2009) 18424–18433. doi:10.1074/jbc.M109.007104.

[10] Y. Demont, C. Corbet, A. Page, Y. Ataman-Önal, G. Choquet-Kastylevsky, I. Fliniaux, X. Le Bourhis, R.-A. Toillon, R.A. Bradshaw, H. Hondermarck, Pro-nerve growth factor induces autocrine stimulation of breast cancer cell invasion through tropomyosin-related kinase A (TrkA) and sortilin protein, J. Biol. Chem. 287 (2012) 1923–1931. doi:10.1074/jbc.M110.211714.

[11] J. Pundavela, Y. Demont, P. Jobling, L.F. Lincz, S. Roselli, R.F. Thorne, D. Bond, R.A. Bradshaw, M.M. Walker, H. Hondermarck, ProNGF correlates with Gleason score and is a potential driver of nerve infiltration in prostate cancer, Am. J. Pathol. 184 (2014) 3156–3162. doi:10.1016/j.ajpath.2014.08.009.

[12] F. Truzzi, A. Marconi, R. Lotti, K. Dallaglio, L.E. French, B.L. Hempstead, C. Pincelli, Neurotrophins and their receptors stimulate melanoma cell

proliferation and migration, J. Invest. Dermatol. 128 (2008) 2031–2040. doi:10.1038/jid.2008.21.
[13] S. Faulkner, S. Roselli, Y. Demont, J. Pundavela, G. Choquet, P. Leissner, C. Oldmeadow, J. Attia, M.M. Walker, H. Hondermarck, ProNGF is a potential diagnostic biomarker for thyroid cancer, Oncotarget. 7 (2016) 28488–28497. doi:10.18632/oncotarget.8652.
[14] W. Song, Y. Hwang, V.M. Youngblood, R.S. Cook, J.M. Balko, J. Chen, D.M. Brantley-Sieders, Targeting EphA2 impairs cell cycle progression and growth of basal-like/triple-negative breast cancers, Oncogene. 36 (2017) 5620–5630. doi:10.1038/onc.2017.170.
[15] L. Aubert, M. Guilbert, C. Corbet, E. Génot, E. Adriaenssens, T. Chassat, F. Bertucci, T. Daubon, N. Magné, X.L. Bourhis, R.-A. Toillon, NGF-induced TrkA/CD44 association is involved in tumor aggressiveness and resistance to lestaurtinib, Oncotarget. 6 (2015) 9807–9819. doi:10.18632/oncotarget.3227.
[16] R.-A. Toillon, C. Lagadec, A. Page, V. Chopin, P.-E. Sautière, J.-M. Ricort, J. Lemoine, M. Zhang, H. Hondermarck, X. Le Bourhis, Proteomics demonstration that normal breast epithelial cells can induce apoptosis of breast cancer cells through insulin-like growth factor-binding protein-3 and maspin, Mol. Cell Proteomics. 6 (2007) 1239–1247. doi:10.1074/mcp.M600477-MCP200.
[17] E. Tomellini, Y. Touil, C. Lagadec, S. Julien, P. Ostyn, N. Ziental-Gelus, S. Meignan, J. Lengrand, E. Adriaenssens, R. Polakowska, X. Le Bourhis, Nerve growth factor and proNGF simultaneously promote symmetric self-renewal, quiescence, and epithelial to mesenchymal transition to enlarge the breast cancer stem cell compartment, Stem Cells. 33 (2015) 342–353. doi:10.1002/stem.1849.
[18] D.P. Zelinski, N.D. Zantek, J.C. Stewart, A.R. Irizarry, M.S. Kinch, EphA2 overexpression causes tumorigenesis of mammary epithelial cells, Cancer Res. 61 (2001) 2301–2306.
[19] L. Faoro, P.A. Singleton, G.M. Cervantes, F.E. Lennon, N.W. Choong, R. Kanteti, B.D. Ferguson, A.N. Husain, M.S. Tretiakova, N. Ramnath, E.E. Vokes, R. Salgia, EphA2 mutation in lung squamous cell carcinoma promotes increased cell survival, cell invasion, focal adhesions, and mammalian target of rapamycin activation, J. Biol. Chem. 285 (2010) 18575–18585. doi:10.1074/jbc.M109.075085.
[20] M.A. Chellaiah, M.D. Schaller, Activation of Src kinase by protein-tyrosine phosphatase-PEST in osteoclasts: comparative analysis of the effects of bisphosphonate and protein-tyrosine phosphatase inhibitor on Src activation in vitro, J. Cell. Physiol. 220 (2009) 382–393. doi:10.1002/jcp.21777.
[21] S. Roselli, Y. Wallez, L. Wang, V. Vervoort, E.B. Pasquale, The SH2 domain protein Shep1 regulates the in vivo signaling function of the scaffolding protein Cas, Cell. Signal. 22 (2010) 1745–1752. doi:10.1016/j.cellsig.2010.06.015.
[22] Y. Zhang, Y. Tu, J. Zhao, K. Chen, C. Wu, Reversion-induced LIM interaction with Src reveals a novel Src inactivation cycle, J. Cell Biol. 184 (2009) 785–792. doi:10.1083/jcb.200810155.
[23] B. Fadeel, E. Grzybowska, HAX-1: a multifunctional protein with emerging roles in human disease, Biochim. Biophys. Acta. 1790 (2009) 1139–1148. doi:10.1016/j.bbagen.2009.06.004.

[24] T.G.P. Grunewald, U. Kammerer, E. Schulze, D. Schindler, A. Honig, M. Zimmer, E. Butt, Silencing of LASP-1 influences zyxin localization, inhibits proliferation and reduces migration in breast cancer cells, Exp. Cell Res. 312 (2006) 974–982. doi:10.1016/j.yexcr.2005.12.016.
[25] M.J. Kean, K.C. Williams, M. Skalski, D. Myers, A. Burtnik, D. Foster, M.G. Coppolino, VAMP3, syntaxin-13 and SNAP23 are involved in secretion of matrix metalloproteinases, degradation of the extracellular matrix and cell invasion, J. Cell. Sci. 122 (2009) 4089–4098. doi:10.1242/jcs.052761.
[26] Y. Matsuoka, X. Li, V. Bennett, Adducin: structure, function and regulation, Cell. Mol. Life Sci. 57 (2000) 884–895. doi:10.1007/PL00000731.
[27] K. Mitchell, K.B. Svenson, W.M. Longmate, K. Gkirtzimanaki, R. Sadej, X. Wang, J. Zhao, A.G. Eliopoulos, F. Berditchevski, C.M. Dipersio, Suppression of integrin alpha3beta1 in breast cancer cells reduces cyclooxygenase-2 gene expression and inhibits tumorigenesis, invasion, and cross-talk to endothelial cells, Cancer Res. 70 (2010) 6359–6367. doi:10.1158/0008-5472.CAN-09-4283.
[28] W. Zhang, B. Jiang, Z. Guo, C. Sardet, B. Zou, C.S.C. Lam, J. Li, M. He, H.-Y. Lan, R. Pang, I.F.N. Hung, V.P.Y. Tan, J. Wang, B.C.Y. Wong, Four-and-a-half LIM protein 2 promotes invasive potential and epithelial-mesenchymal transition in colon cancer, Carcinogenesis. 31 (2010) 1220–1229. doi:10.1093/carcin/bgq094.
[29] M.S. Ioannou, M. Fahnestock, ProNGF, but Not NGF, Switches from Neurotrophic to Apoptotic Activity in Response to Reductions in TrkA Receptor Levels, Int J Mol Sci. 18 (2017). doi:10.3390/ijms18030599.
[30] B. Davidson, R. Reich, P. Lazarovici, V. Ann Flørenes, S. Nielsen, J.M. Nesland, Altered expression and activation of the nerve growth factor receptors TrkA and p75 provide the first evidence of tumor progression to effusion in breast carcinoma, Breast Cancer Res. Treat. 83 (2004) 119–128. doi:10.1023/B:BREA.0000010704.17479.8a.
[31] O. Shonukan, I. Bagayogo, P. McCrea, M. Chao, B. Hempstead, Neurotrophin-induced melanoma cell migration is mediated through the actin-bundling protein fascin, Oncogene. 22 (2003) 3616–3623. doi:10.1038/sj.onc.1206561.
[32] E.B. Pasquale, Eph-ephrin bidirectional signaling in physiology and disease, Cell. 133 (2008) 38–52. doi:10.1016/j.cell.2008.03.011.
[33] W.B. Fang, R.C. Ireton, G. Zhuang, T. Takahashi, A. Reynolds, J. Chen, Overexpression of EPHA2 receptor destabilizes adherens junctions via a RhoA-dependent mechanism, J. Cell. Sci. 121 (2008) 358–368. doi:10.1242/jcs.017145.
[34] N. Hiramoto-Yamaki, S. Takeuchi, S. Ueda, K. Harada, S. Fujimoto, M. Negishi, H. Katoh, Ephexin4 and EphA2 mediate cell migration through a RhoG-dependent mechanism, J. Cell Biol. 190 (2010) 461–477. doi:10.1083/jcb.201005141.
[35] H. Miao, D.-Q. Li, A. Mukherjee, H. Guo, A. Petty, J. Cutter, J.P. Basilion, J. Sedor, J. Wu, D. Danielpour, A.E. Sloan, M.L. Cohen, B. Wang, EphA2 mediates ligand-dependent inhibition and ligand-independent promotion of cell migration and invasion via a reciprocal regulatory loop with Akt, Cancer Cell. 16 (2009) 9–20. doi:10.1016/j.ccr.2009.04.009.
[36] Y. Zhou, N. Yamada, T. Tanaka, T. Hori, S. Yokoyama, Y. Hayakawa, S. Yano, J. Fukuoka, K. Koizumi, I. Saiki, H. Sakurai, Crucial roles of RSK in cell

motility by catalysing serine phosphorylation of EphA2, Nat Commun. 6 (2015) 7679. doi:10.1038/ncomms8679.
[37] S.M. MacGrath, A.J. Koleske, Cortactin in cell migration and cancer at a glance, J Cell Sci. 125 (2012) 1621–1626. doi:10.1242/jcs.093781.
[38] K. Berns, R. Bernards, Understanding resistance to targeted cancer drugs through loss of function genetic screens, Drug Resist. Updat. 15 (2012) 268–275. doi:10.1016/j.drup.2012.10.002.
[39] J.M. Stommel, A.C. Kimmelman, H. Ying, R. Nabioullin, A.H. Ponugoti, R. Wiedemeyer, A.H. Stegh, J.E. Bradner, K.L. Ligon, C. Brennan, L. Chin, R.A. DePinho, Coactivation of receptor tyrosine kinases affects the response of tumor cells to targeted therapies, Science. 318 (2007) 287–290. doi:10.1126/science.1142946.
[40] G. Zhuang, D.M. Brantley-Sieders, D. Vaught, J. Yu, L. Xie, S. Wells, D. Jackson, R. Muraoka-Cook, C. Arteaga, J. Chen, Elevation of receptor tyrosine kinase EphA2 mediates resistance to trastuzumab therapy, Cancer Res. 70 (2010) 299–308. doi:10.1158/0008-5472.CAN-09-1845.
[41] K.R. Amato, S. Wang, L. Tan, A.K. Hastings, W. Song, C.M. Lovly, C.B. Meador, F. Ye, P. Lu, J.M. Balko, D.C. Colvin, J.M. Cates, W. Pao, N.S. Gray, J. Chen, EPHA2 Blockade Overcomes Acquired Resistance to EGFR Kinase Inhibitors in Lung Cancer, Cancer Res. 76 (2016) 305–318. doi:10.1158/0008-5472.CAN-15-0717.

TABLE

Table 1: Correlation between expression levels of TrkA and EphA2, TrkA/EphA2 association (PLA signal) and clinical parameters of patient samples

		TrkA	EphA2	TrkA/EphA2 PLA
Estrogen receptor	**Positive (n=109)**	1.725±0.09478 p= 0.1408	1.817±0.1011 p=0.2155	2.193±0.1169 p=0.1608
	Negative (n=71)	1.944±0.1115	2.014±0.1212	1.915±0.1615
Progesterone receptor	**Positive (n=95)**	**1.663±0.09996 p=0.0318**	1.758±0.1097 p=0.0536	2.053±0.1201 p=0.5557
	Negative (n=84)	**1.976±0.1044**	2.060±0.1089	2.141±0.1541
HER-2	**Positive (n=69)**	1.783±0.1254 p=0.8799	1.884±0.1248 p=0.9606	2.217±0.1650 p=0.2717
	Negative (n=113)	1.805±0.08876	1.876±0.09988	2.000±0.1166
Triple negative	**Positive (n=34)**	2.088±0.1544 p=0.0578	2.176±0.1661 p=0.0715	1.765±0.2315 p=0.1053
	Negative (n=147)	1.735±0.08153	1.816±0.08743	2.163±0.1049
Lymph node invasion	**Positive (n=116)**	1.724±0.09372 p=0.1166	1.897±0.09976 p=0.9171	2.138±0.1193 p=0.2127
	Negative (n=69)	1.957±0.1081	1.913±0.1181	1.899±0.1193

FIGURE LEGENDS

Figure 1: Proteomic analysis of HA-TrkA partners revealed EphA2 association and downstream signaling pathways proteins. (A) MDA-MB-231 HA-TrkA cells were treated in absence or presence of non-cleavable proNGF (0.5nM) for 5 and 30 min. Total cell lysates were subjected to HA immunoprecipitation and separated in 10% SDS-PAGE. Proteins were revealed by colloidal blue Coomassie staining. Using transilluminator, intensity of bands was appreciated by CC and R-A T and bands with stronger intensity than that of control were cut (red square). Protein peptide digests were then subjected to mass spectrometry analysis. **(B)** Identified proteins were analyzed for Biological pathways using Panther software. **(C)** Mass spectrometry identification of selected putative interacting partners of TrkA under proNGF stimulation (5 or 30 min). For each identified protein, the Uniprot ID, the number and sequence of the different peptides allowing protein identification and the individual peptide Mascot score are summarized. Underlined amino-acids (C and M) are oxidized residues. MW: Molecular Weight. GO: Gene Ontology.

Figure 2: ProNGF induced association of sortilin, TrkA and EphA2. **(A)** Representative immunoblotting for sortilin, EphA2 and TrkA following IP anti-HA (TrkA), sortilin or EphA2 in HA-TrkA MDA-MB-231 cells after non-cleavable proNGF treatment. **(B-E)** Representative pictures (B and D) and quantification (C and E) for sortilin/TrkA (B and C) and TrkA/EphA2 (D and E) PLA signals in HA-TrkA MDA-MB-231 cells after non-cleavable proNGF treatment. PLA signals were quantified on three independent experiments. In (C) and (E), data are expressed as scatter plots. ***p<0.001; ns, not significant.

651

652 **Figure 3: ProNGF-induced association of TrkA with sortilin and EphA2 was**
653 **sequential.**

654 **(A-B)** Representative immunoblotting for sortilin, EphA2 and TrkA after IP anti-HA
655 (TrkA) following treatment with 1 µM neurotensin (A) or after IP anti-sortilin in cells
656 transfected with TrkA-targeting siRNA (B). **(C)** Representative pictures of
657 sortilin/EphA2 PLA. **(D-E)** Representative immunoblotting for sortilin, EphA2 and
658 TrkA after IP anti-HA in HA-TrkA MDA-MB-231 cells expressing a kinase-dead
659 TrkA mutant (D) or transfected with EphA2-targeting siRNA (E). In (D), TrkA
660 phosphorylation in the kinase domain (Y674/675 residues) was also evaluated by
661 immunoblotting. **(F-G)** Representative immunoblotting for the phosphorylated and
662 total forms of Akt and Src in non-cleavable proNGF-stimulated HA-TrkA MDA-MB-
663 231 cells expressing a kinase-dead TrkA mutant (F) or cells transfected with
664 EphA2-targeting siRNA (G). Immunoprecipitations and immunoblots were carried
665 out at least 2 times with similar results. **(H)** Putative dynamic of proNGF-induced
666 sortilin/TrkA/EphA2 signaling in breast cancer cells. After proNGF binding to
667 sortilin (1), TrkA is phosphorylated allowing Akt activation (2). Additionally, EphA2
668 is also recruited to the sortilin/TrkA complex in a TrkA kinase-independent manner,
669 leading to Src activation (3).

670

671 **Figure 4: TrkA/EphA2 complex was involved in proNGF-stimulated**
672 **clonogenic cell growth. (A)** PLA of TrkA/EphA2 complex in wild-type MDA-MB-
673 231, SUM159-PT, MCF-7, T-47D and HCC-1954 breast cancer cells following
674 proNGF treatment (5 and 30 min). **(B)** Clonogenic cell growth following proNGF
675 treatment (5 and 30 min) and transfection of EphA2-targeting siRNA. **(C)**

Clonogenic cell growth of MDA-MB-231 cells following treatment with 10 nM K252a and/or transfection with EphA2-targeting siRNA. Data are expressed as scatter plots (A) or means ± SEM (B-C). **p<0.01; ***p<0.001; ns, not significant.

Figure 5: Combinatorial treatment with TrkA- and EphA2-targeting modalities delays primary tumor growth and metastasis formation. **(A-B)** Tumor growth of MDA-MB-231 xenografts in SCID mice submitted to 3 injections (every 3 days; black arrows) of either *in vivo* JetPEI + control or EphA2-targeting siRNA (7.5 µg/mouse), or CEP-701 (10 mg/kg) alone or in combination. Tumor volumes were measured at different intervals (A) and represented as scatter plots at the end of the experiment (B). (**C**) Detection of metastatic human breast cancer cells (as determined by RT-PCR for the expression of the human microglobulin) in different organs (lungs, liver and brain) of MDA-MB-231 xenograft-bearing mice submitted to 5 injections (every 3 days; black arrows) of either *in vivo* JetPEI + control or EphA2-targeting siRNA (7.5 µg/mouse), or CEP-701 (10 mg/kg) alone or in combination. *p<0.05; **p<0.01; ***p<0.001; ns: not significant. Data are expressed as means ± SEM (A) or scatter plots (B).

Figure 6: TrkA/EphA2 complex expression is associated with overall survival (OS) decrease for breast cancer patients. (A-C) Representative pictures for TrkA immunostaining in breast tumors, defined as low (A), medium (B) or high (C). **(D)** Kaplan-Meier OS curves in breast cancer patients according to TrkA staining. **(E-G)** Representative pictures for EphA2 immunostaining in breast tumors, defined as low (E), medium (F) or high (G). **(H)** Kaplan-Meier OS curves in breast cancer patients according to EphA2 staining. **(I-K)** Representative PLA images depicting

low (I), medium (J) and high staining (K) for TrkA/EphA2 complex on patient breast tumor samples. **(L)** Kaplan-Meier OS curves in breast cancer patients according to TrkA/EphA2 complex abundance.

A

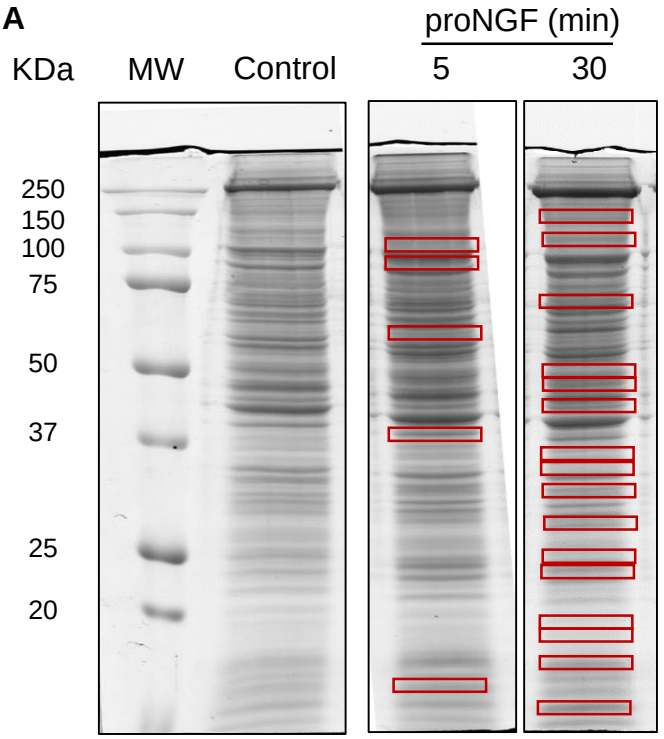

B

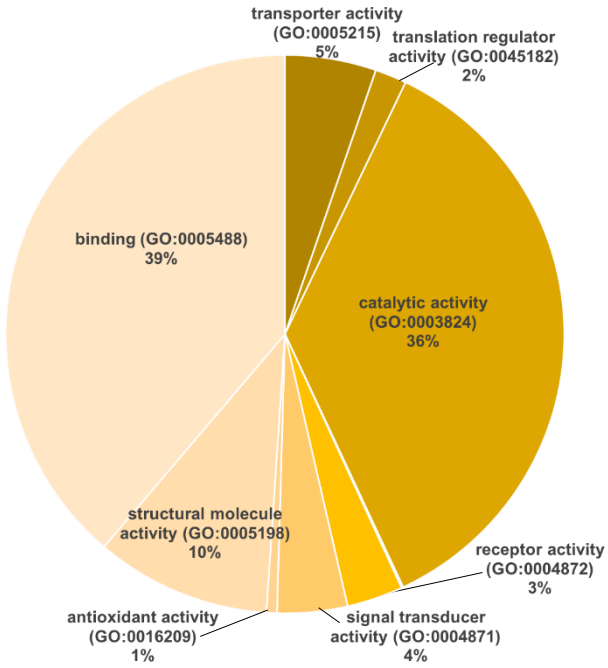

C

Protein name	Uniprot ID	Peptide sequences	Mascot score
Sortilin	Q99523	IYSFGLGGR	31
EphA2	P29317	FADIVSILDK	45
		TVSEWLESIK	25
Src	P12931	AANILVGENLVCK	54
Cortactin	Q14247	VDQSAVGFEYQGK	44
		YGLFPANYVELR	84
p130 Cas	P56945	LVFIGDTLSR	33
		ATAPGPEGGGTLHPNPTDK	20
SHEP1	Q8N5H7	TEGTK	30
		LDLLER	39
PTP-PEST	Q05209	TLLLEFQNESR	55
RIL	P50479	GYFFLDER	46
		DFSAPLTISR	25
		VKPPEGYDVVAVYPNAK	17
Lasp1	Q14847	GFSVVADTPELQR	60
SNAP23	O00161	ILGLAIESQDAGIK	76
FHL2	Q14192	CSLSLVGR	59
		YISFEER	43
		NSLVDKPFAAK	24
		CAGCTNPISGLGGTK	26
		GSSWHETCFICHR	54
		DDFAYCLNCFCDLYAK	61
		EDQLLCTDCYSNEYSSK	29
HAX1	O00165	IFGGVLESDAR	38
adducin	P35611	INLQGDIVDR	49
MARCKS	P29966	LSGFSFK	31
		GEPAAAAAPEAGASPVEK	26
		EAPAEGEAAEPGSPTAAEGEA ASAASSTSSPK	86
Gelsolin	P06396	AGALNSNDAFVLK	41
Integrin alpha-3	P26006	YLLLAGAPR	23
		TVEDVGSPLK	34
		LELLLMDNLR	26
		LELLLMDNLR	41
		EAGNPGSLFGYSVALHR	27
Integrin beta-1	P05556	IGFGSFVEK	64
		LLVFSTDAGFHFAGDGK	63

Lévêque *et al.*, Figure 1

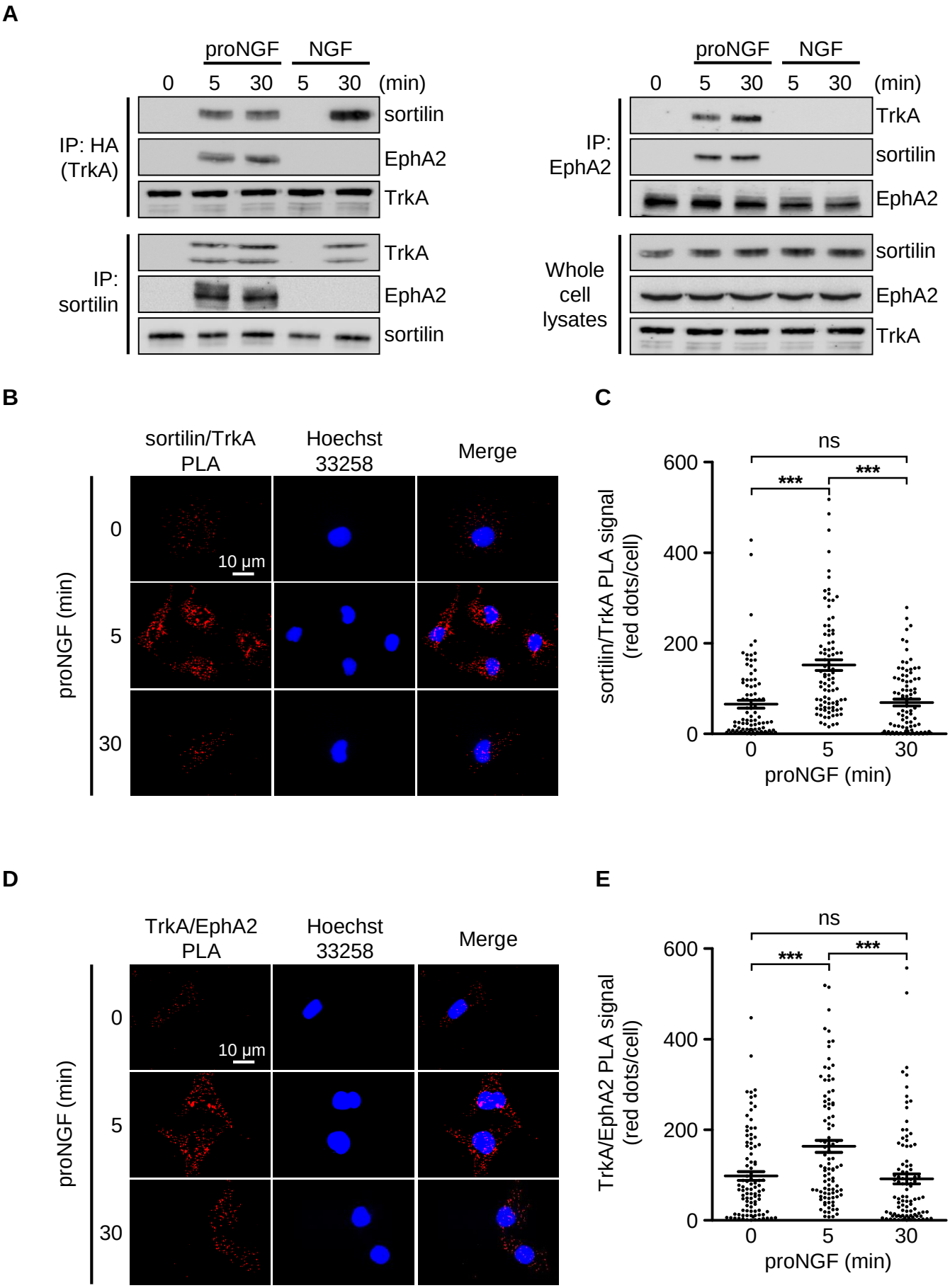

Lévêque *et al.*, Figure 2

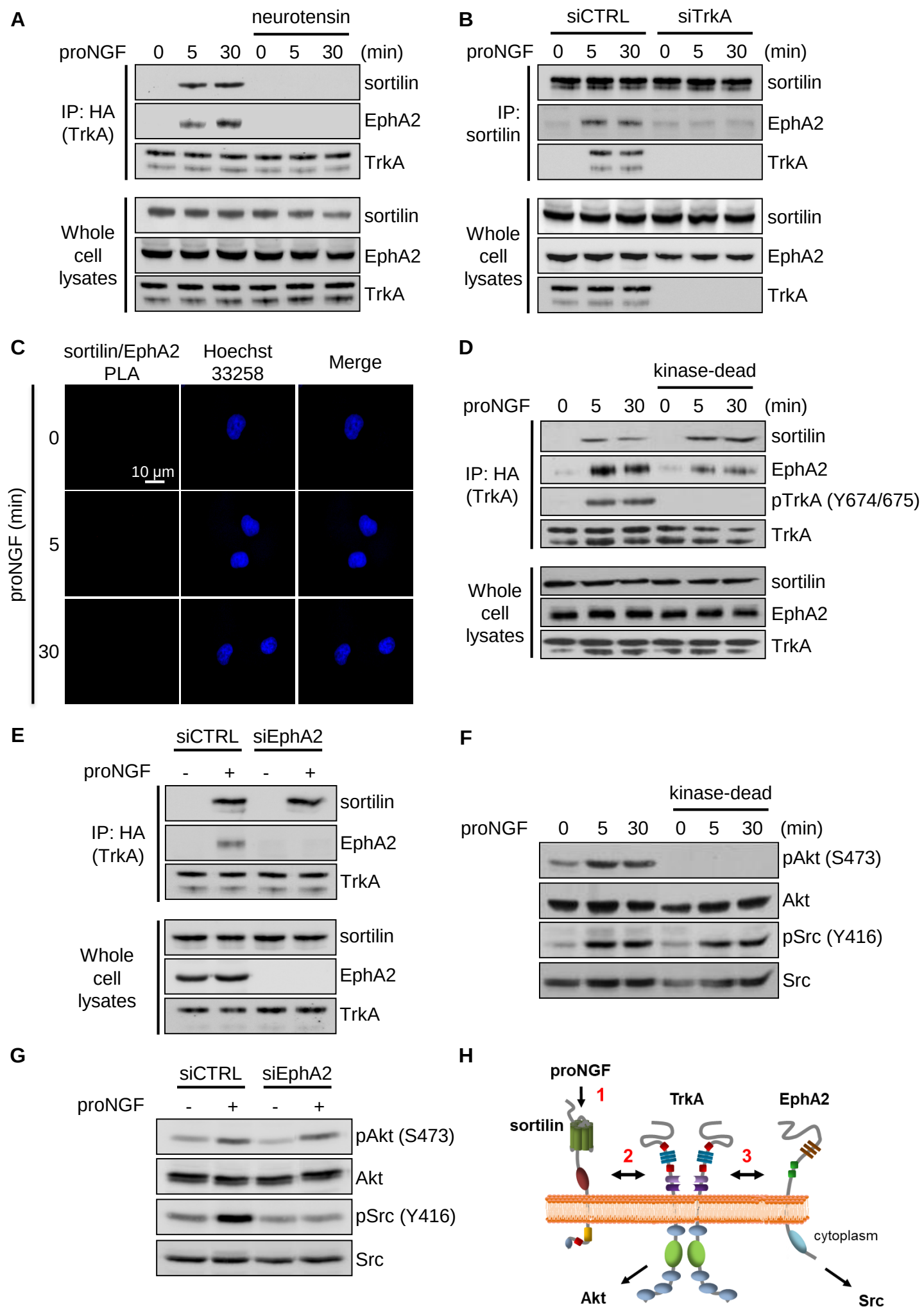

Lévêque *et al.*, Figure 3

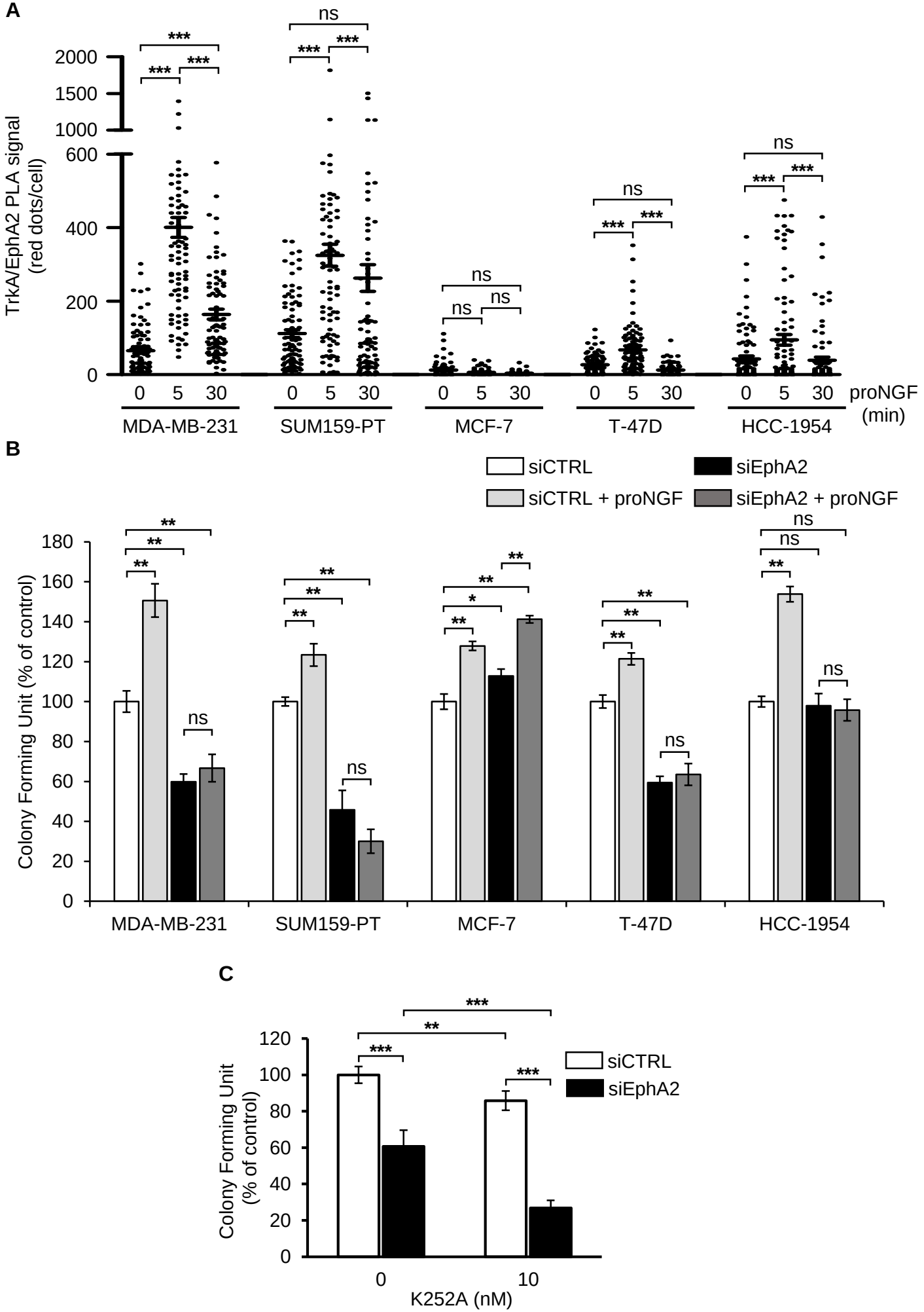

Lévêque *et al.*, Figure 4

A

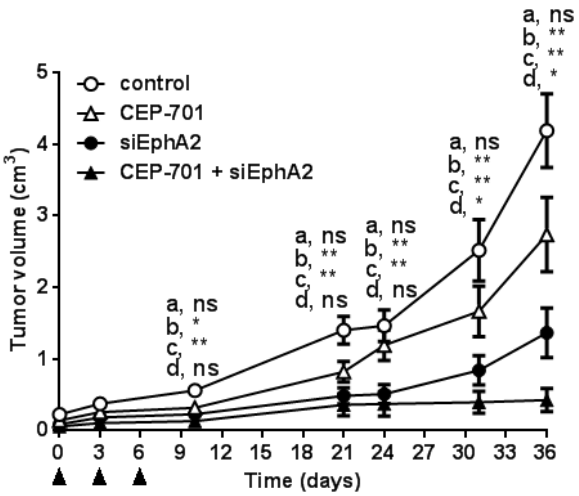

B

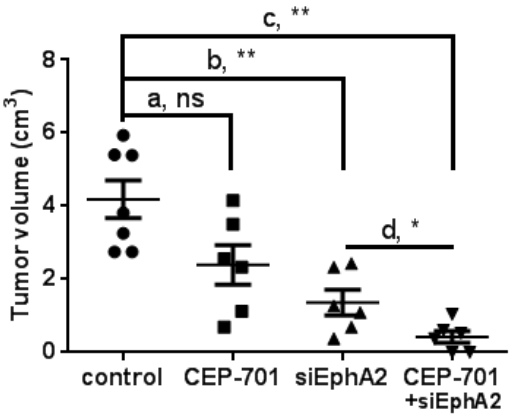

C

Metastasis in mice	siCTRL	siTrkA	siEphA2	siTrkA+siEphA2
Lung	10/10	10/10	10/10	10/10
Liver	7/10	4/10	7/10	4/10
Brain	8/10	8/10	7/10	4/10

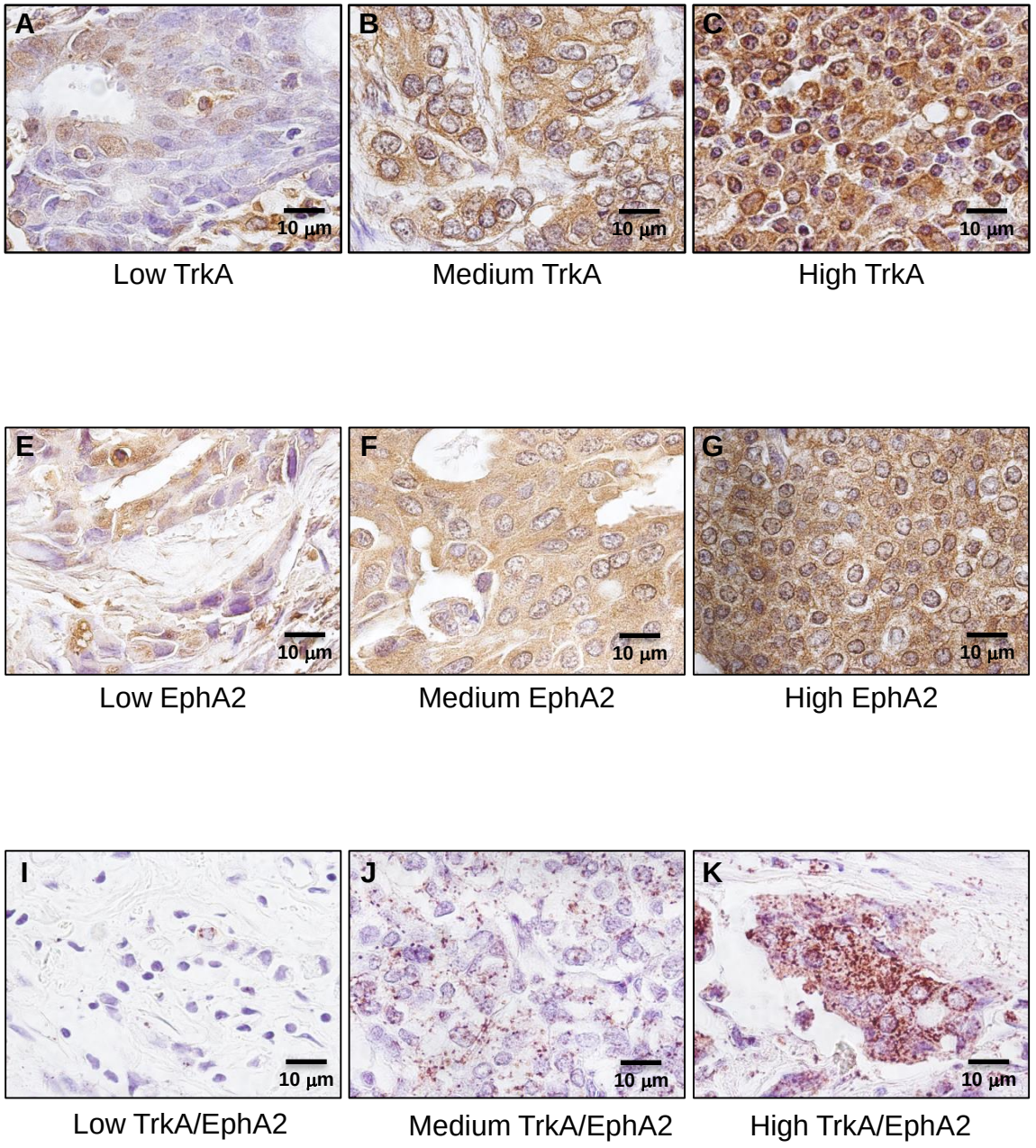

Lévêque *et al.*, Figure 6